

# Characterizing rheological properties and microstructure of thioester networks during degradation

Shivani Desai<sup>a</sup>, Benjamin J. Carberry<sup>b</sup>, Kristi S. Anseth<sup>b</sup>, and  
Kelly M. Schultz<sup>\*a</sup>

<sup>a</sup>Department of Chemical and Biomolecular Engineering, Lehigh  
University, Bethlehem, PA, USA. \* Tel: +1 610 758 2012; E-mail:  
kes513@lehigh.edu

<sup>b</sup>Department of Chemical and Biological Engineering, University of  
Colorado at Boulder, Boulder, CO, USA.

## Supporting Information

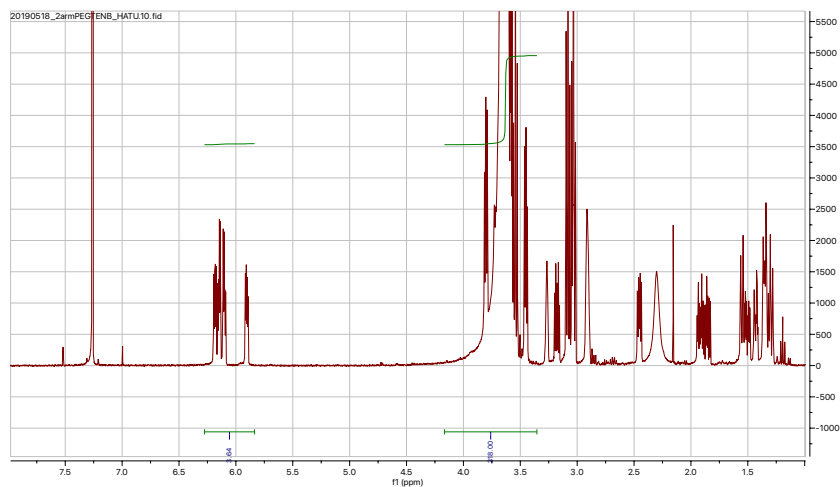


Fig. S1: Nuclear magnetic resonance spectrum of 3.5 *kDa* Poly(ethylene glycol)-thioester norbornene in  $\text{CDCl}_3$  (400 *Hz*)  $\delta$  6.29–5.82 (m, 2H), 3.99–3.42 (m, 1818H)

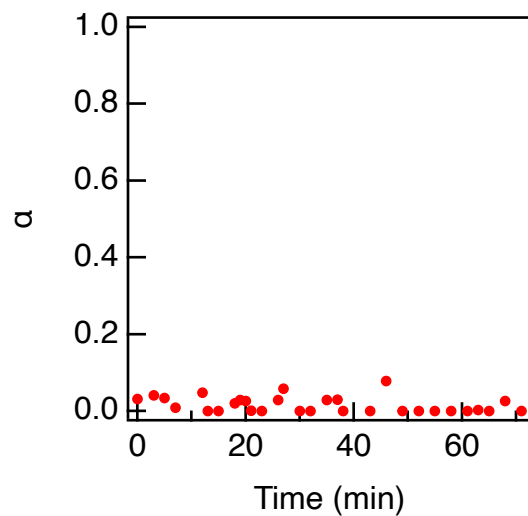


Fig. S2: Networks with 50% excess thiol degraded with 0.1 *M* L-cysteine. This network does not degrade in this concentration of L-cysteine solution.

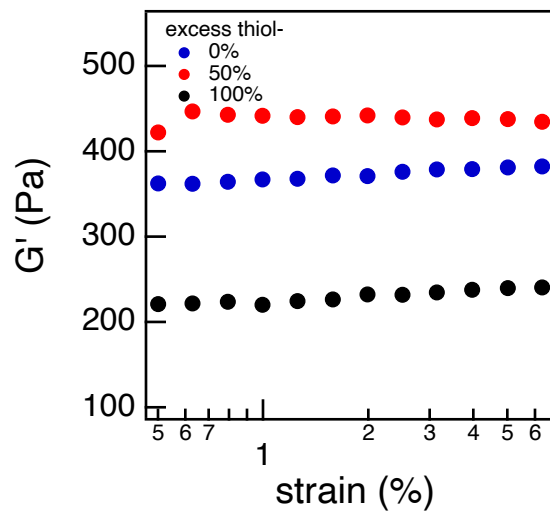


Fig. S3: Strain sweeps of PEG-thioester norbornene CANs. Strain sweeps are used to identify the linear viscoelastic regime. A strain sweep is used to measure all scaffolds between 0.5% and 10% strain at a frequency of 1 *Hz*. From these measurements, 1% strain is chosen for frequency sweep measurements in the linear viscoelastic regime.

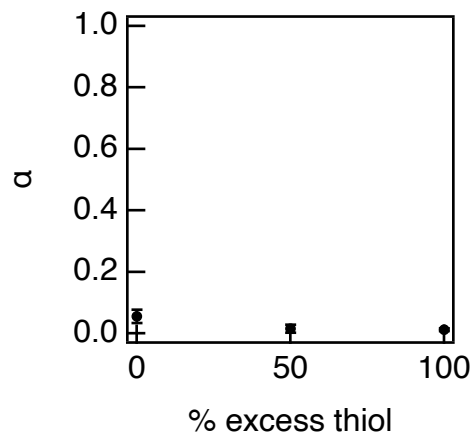


Fig. S4: The values of the logarithmic slope of the MSD,  $\alpha = \frac{d \log \langle \Delta r^2(\tau) \rangle}{d \log \tau}$ , for each network composition before incubating in L-cysteine solution.  $\alpha \approx 0$  for all network compositions which is a measure of particles completely arrested in a gel network.

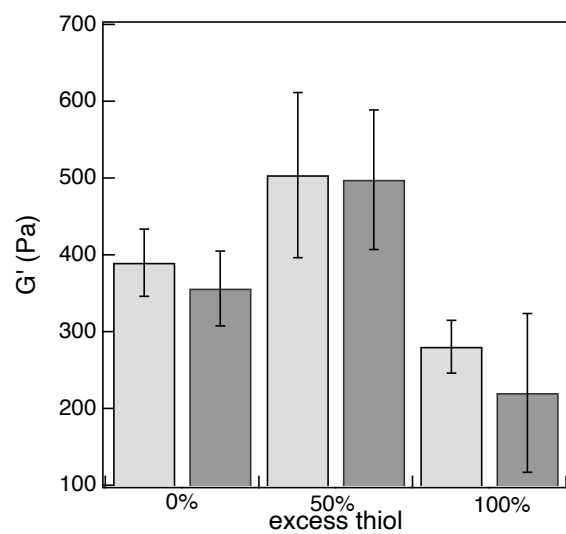


Fig. S5: Measurements of each CAN composition before and after incubation in  $1\times$  PBS for 3 *hours*. Light gray bars are the elastic moduli of unswollen hydrogels and dark gray bars are the elastic moduli of thioester networks after incubating for 3 *hrs* in  $1\times$  PBS. The elastic modulus,  $G'$ , of thioester networks does not change.

## Time-cure superposition

Networks with 0% excess thiol

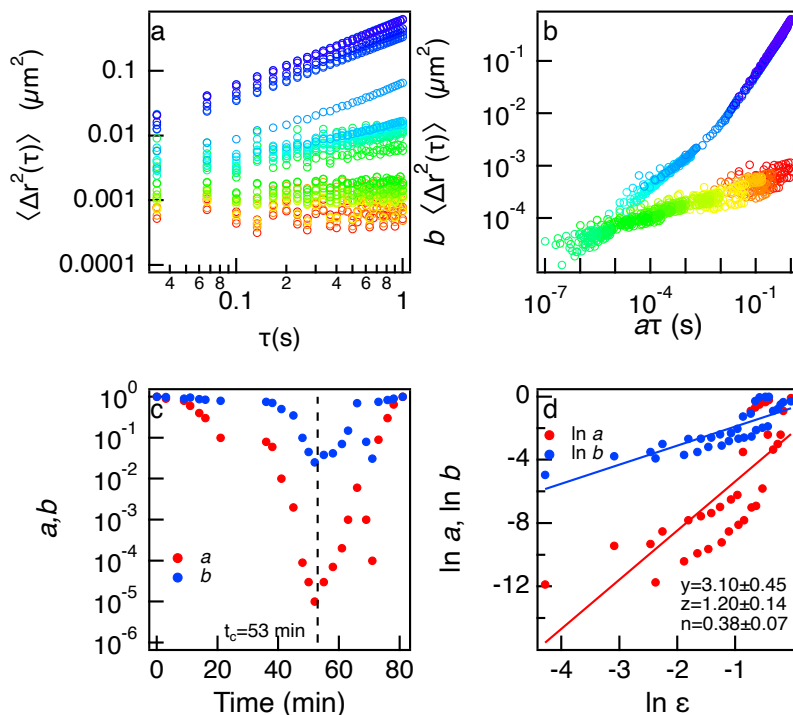


Fig. S6: Time-cure superposition of PEG-thioester networks with 0% excess thiol (second replicate experiment). (a) MSDs are measured during degradation of networks with 0% excess thiol. (b) MSDs are shifted into sol and gel master curves using shift factors  $a$  and  $b$ . (c) Shift factors  $a$  and  $b$  approach zero at  $t_c = 53 \text{ mins}$ . (d)  $y$  and  $z$  are calculated by plotting the logarithm of shift factors  $a$  and  $b$  against the logarithm of distance away from critical degradation time,  $\epsilon = \frac{|t-t_c|}{t_c}$ . The critical relaxation exponent,  $n$ , is calculated from scaling exponents  $y$  and  $z$ .

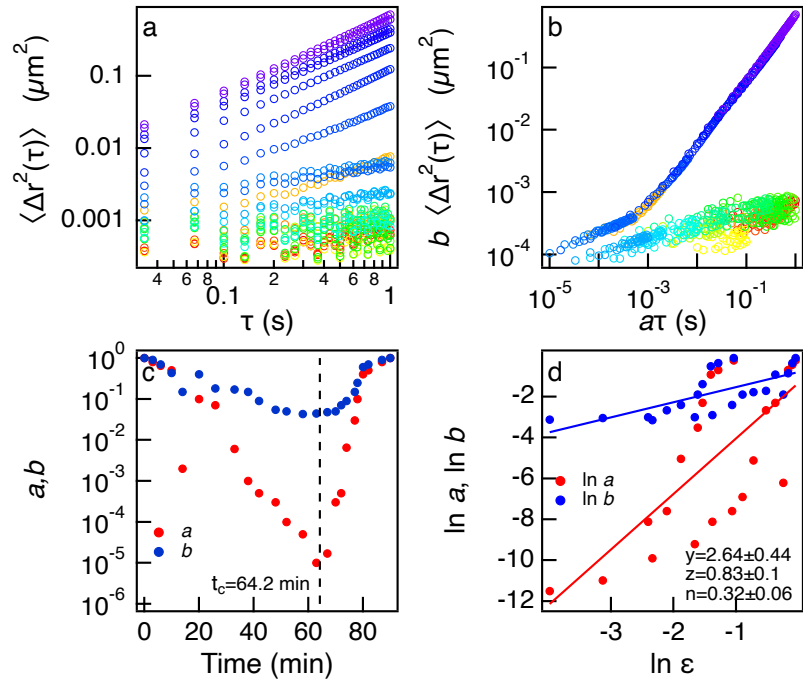


Fig. S7: Time-cure superposition of PEG-thioester networks with 0% excess thiol (third replicate experiment). (a) MSDs are measured during degradation of networks with 0% excess thiol. (b) MSDs are shifted into sol and gel master curves using shift factors  $a$  and  $b$ . (c) Shift factors  $a$  and  $b$  approach zero at  $t_c = 64.2$  mins. (d)  $y$  and  $z$  are calculated by plotting the logarithm of shift factors  $a$  and  $b$  against the logarithm of distance away from critical degradation time,  $\epsilon$ . The critical relaxation exponent,  $n$ , is calculated from scaling exponents  $y$  and  $z$ .

### Networks with 50% excess thiol

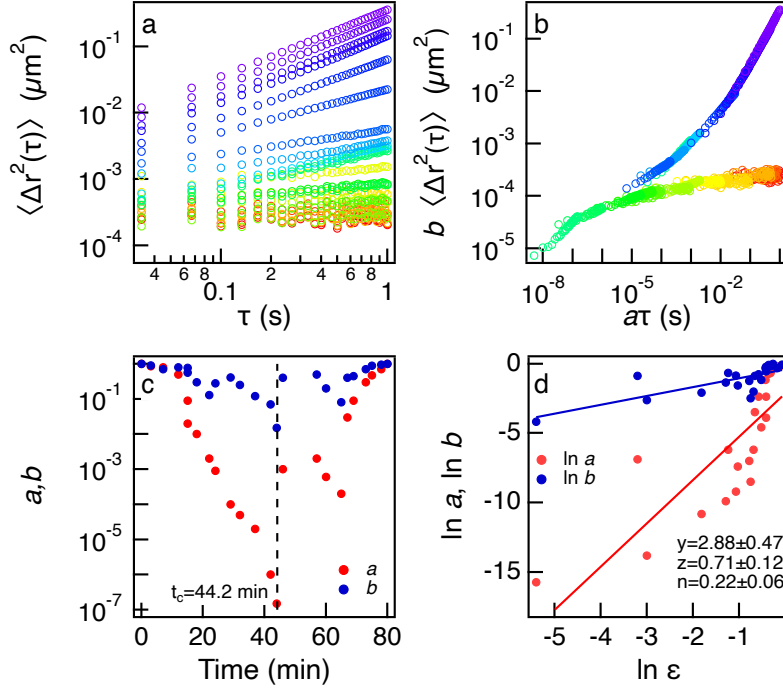


Fig. S8: Time-cure superposition of PEG-thioester networks with 50% excess thiol (first replicate experiment). (a) MSDs are measured during degradation of networks with 50% excess thiol with particles coated in BSA. (b) MSDs are shifted into sol and gel master curves using shift factors  $a$  and  $b$ . (c) Shift factors  $a$  and  $b$  approach zero at  $t_c = 44.2$  mins. (d)  $y$  and  $z$  are calculated by plotting the logarithm of shift factors  $a$  and  $b$  against the logarithm of distance away from critical degradation time,  $\epsilon$ . The critical relaxation exponent,  $n$ , is calculated from scaling exponents  $y$  and  $z$ .

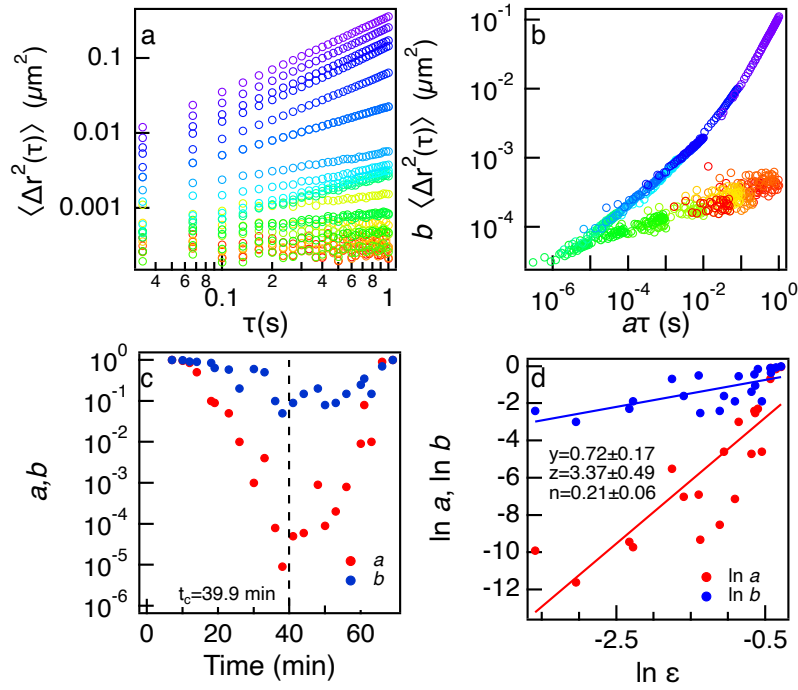


Fig. S9: Time-cure superposition of PEG-thioester networks with 50% excess thiol (second replicate experiment). (a) MSDs are measured during degradation of networks with 50% excess thiol with particles coated in BSA. (b) MSDs are shifted into sol and gel master curves using shift factors  $a$  and  $b$ . (c) Shift factors  $a$  and  $b$  approach zero at  $t_c = 39.9$  mins. (d)  $y$  and  $z$  are calculated by plotting the logarithm of shift factors  $a$  and  $b$  against the logarithm of distance away from critical degradation time,  $\epsilon$ . The critical relaxation exponent,  $n$ , is calculated from scaling exponents  $y$  and  $z$ .



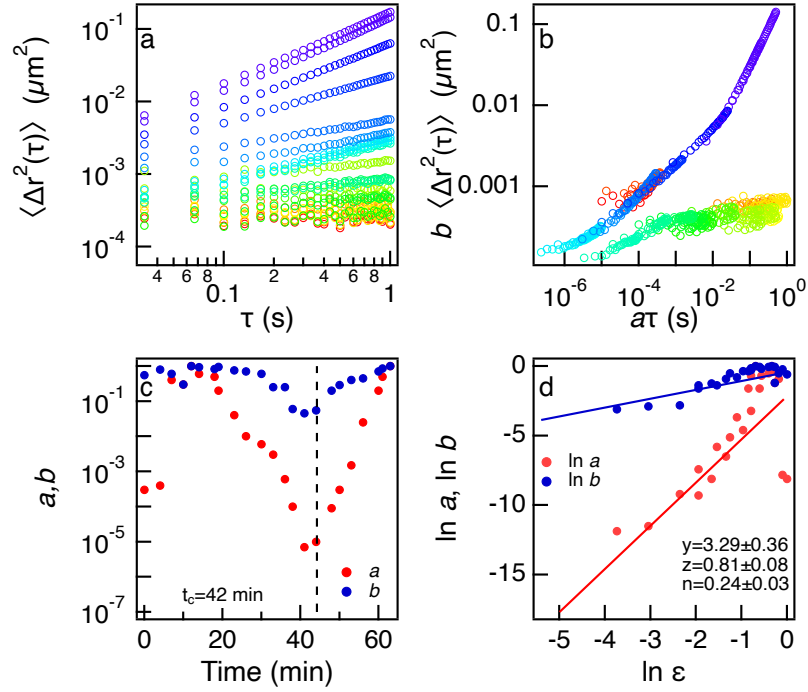


Fig. S10: Time-cure superposition of PEG-thioester networks with 50% excess thiol (third replicate experiment). (a) MSDs are measured during degradation of networks with 50% excess thiol with PEGylated particles. (b) MSDs are shifted into sol and gel master curves using shift factors  $a$  and  $b$ . (c) Shift factors  $a$  and  $b$  approach zero at  $t_c = 42$  mins. (d)  $y$  and  $z$  are calculated by plotting the logarithm of shift factors  $a$  and  $b$  against the logarithm of distance away from critical degradation time,  $\epsilon$ . The critical relaxation exponent,  $n$ , is calculated from scaling exponents  $y$  and  $z$ .

Networks with 100% excess thiol

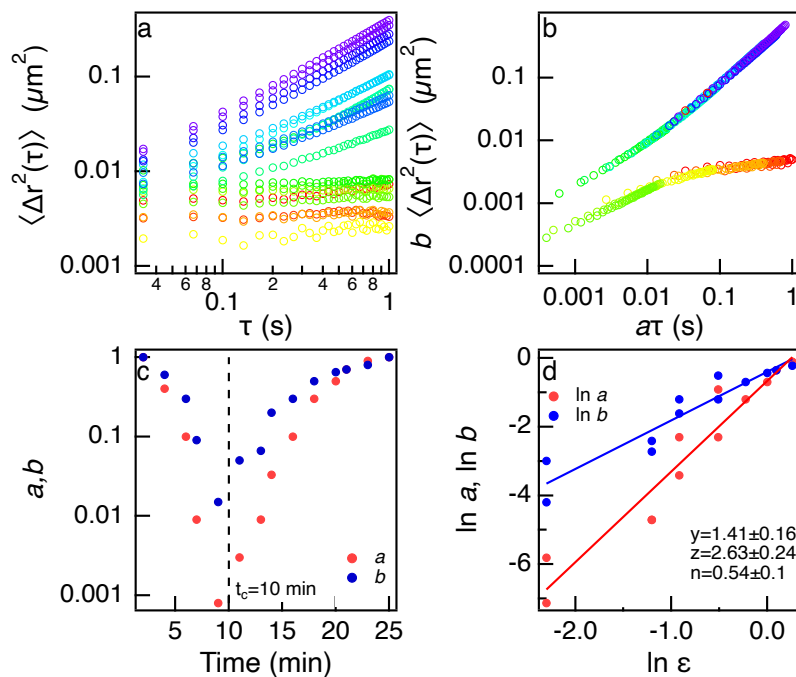


Fig. S11: Time-cure superposition of PEG-thioester networks with 100% excess thiol (first replicate experiment). (a) MSDs are measured during degradation of networks with 100% excess thiol. (b) MSDs are shifted into sol and gel master curves using shift factors  $a$  and  $b$ . (c) Shift factors  $a$  and  $b$  approach zero at  $t_c = 10$  mins. (d)  $y$  and  $z$  are calculated by plotting the logarithm of shift factors  $a$  and  $b$  against the logarithm of distance away from critical degradation time,  $\epsilon$ . The critical relaxation exponent,  $n$ , is calculated from scaling exponents  $y$  and  $z$ .

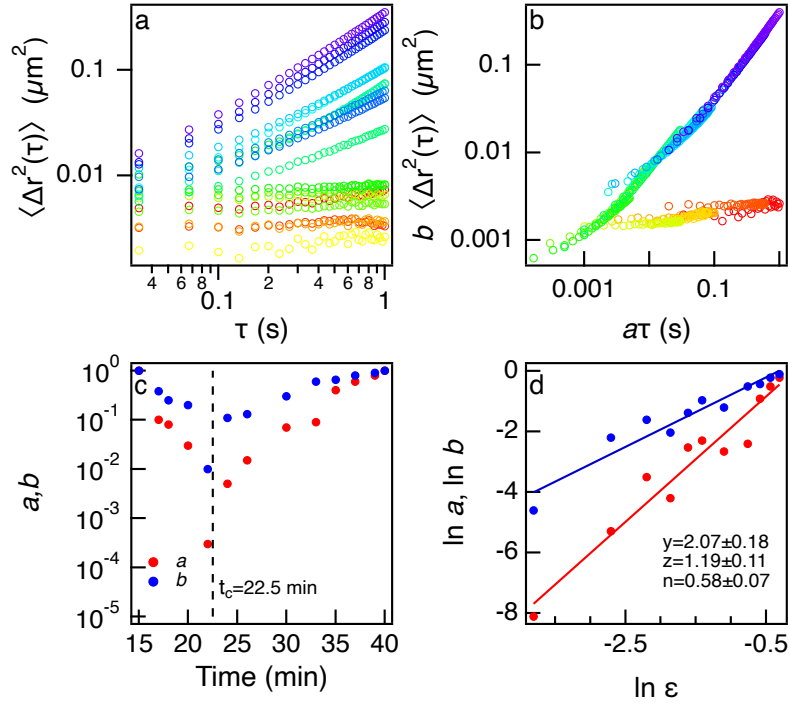


Fig. S12: Time-cure superposition of PEG-thioester networks with 100% excess thiol (second replicate experiment). (a) MSDs are measured during degradation of networks with 100% excess thiol. (b) MSDs are shifted into sol and gel master curves using shift factors  $a$  and  $b$ . (c) Shift factors  $a$  and  $b$  approach zero at  $t_c = 22.5$  mins. (d)  $y$  and  $z$  are calculated by plotting the logarithm of shift factors  $a$  and  $b$  against the logarithm of distance away from critical degradation time,  $\epsilon$ . The critical relaxation exponent,  $n$ , is calculated from scaling exponents  $y$  and  $z$ .

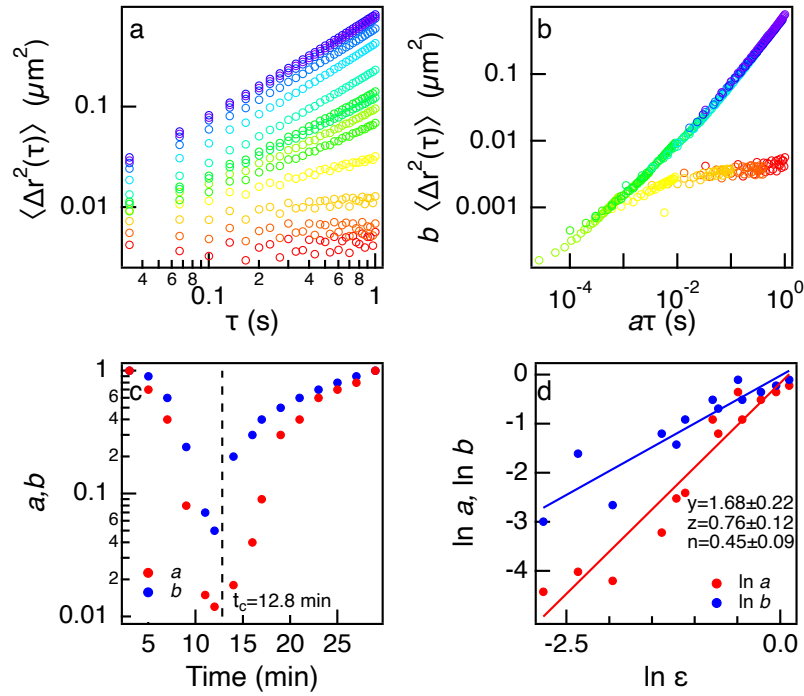


Fig. S13: Time-cure superposition of PEG-thioester networks with 100% excess thiol (third replicate experiment). (a) MSDs are measured during the degradation of networks with 100% excess thiol. (b) MSDs are shifted into sol and gel master curves using shift factors  $a$  and  $b$ . (c) Shift factors  $a$  and  $b$  approach zero at  $t_c = 12.8$  mins. (d)  $y$  and  $z$  are calculated by plotting the logarithm of shift factors  $a$  and  $b$  against the logarithm of distance away from critical degradation time,  $\epsilon$ . The critical relaxation exponent,  $n$ , is calculated from scaling exponents  $y$  and  $z$ .

Networks with 0% excess thiol degraded with a second concentration of L-cysteine

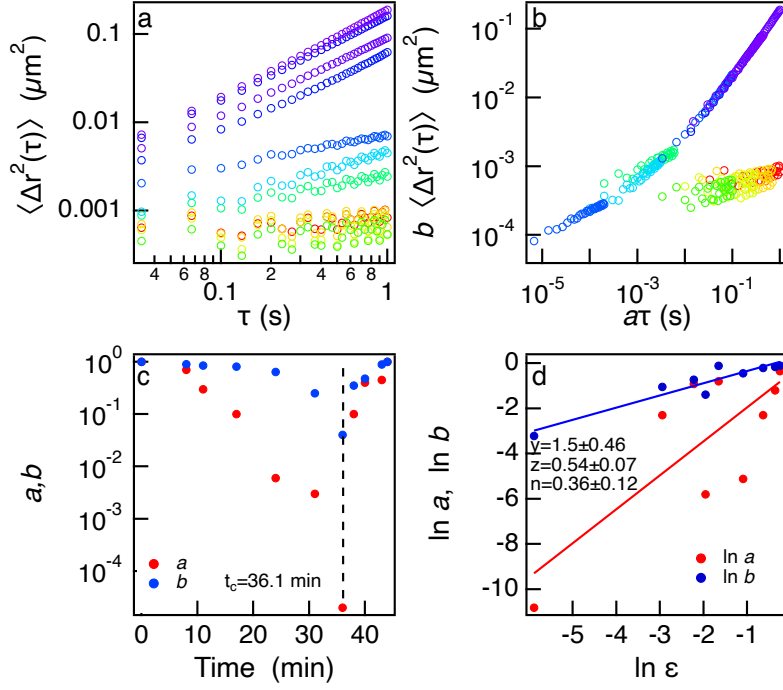


Fig. S14: TCS analysis of 0% excess thiol networks degraded with 0.2 M L-cysteine shows the value of  $n$  does not change when the concentration of L-cysteine is changed. (a) MSDs are measured during the degradation of networks with 0% excess thiol. (b) MSDs are shifted into sol and gel master curves using shift factors  $a$  and  $b$ . (c) Shift factors  $a$  and  $b$  approach zero at  $t_c = 36.1$  mins. (d)  $y$  and  $z$  are calculated by plotting the logarithm of shift factors  $a$  and  $b$  against the logarithm of distance away from critical degradation time. The critical relaxation exponent,  $n$ , is calculated from the scaling exponents  $y$  and  $z$ .

## MPT characterization of all three network compositions

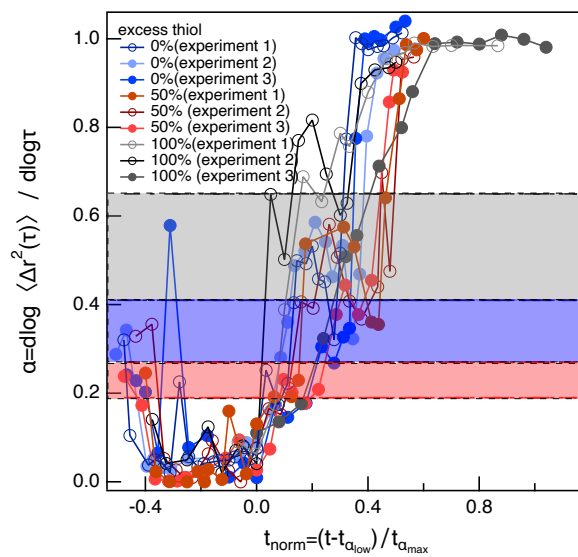


Fig. S15: Thioester networks with 0%, 50% and 100% excess thiol undergo rearrangement during degradation with L-cysteine. Network rearrangement in all three networks is compared by plotting the values of the logarithmic slope of the MSD,  $\alpha$ , during degradation against normalized time,  $t_{norm} = \frac{t - t_{\alpha_{low}}}{t_{\alpha_{max}}}$  where  $t$  is the time data are collected,  $t_{\alpha_{low}}$  is the time when the value of  $\alpha$  starts to increase and  $t_{\alpha_{max}}$  is the time when  $\alpha$  is a maximum.

## Rheological and spatial heterogeneity analysis of MPT data of degradation of all three network compositions

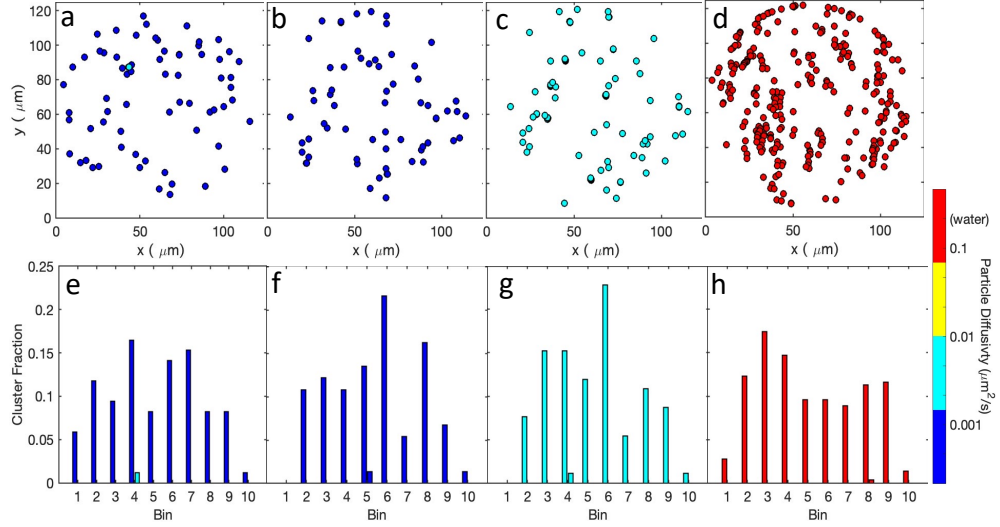


Fig. S16: Fig. S16 (a-d) Rheological and (e-h) spatial heterogeneity in the microenvironments particles are probing during degradation of 0% excess thiol. (a-d) Particle diffusivity is plotted at the starting position of the probe particle, color indicates the diffusivity. (e-h) Histograms of the diffusivity of probe particles along the  $x$ -axis, measuring spatial heterogeneity. Each bin is  $12.5 \mu\text{m}$  in size. Each column of probe diffusivity and spatial heterogeneity is measured at a different time relative to the critical degradation time. This relative time,  $t_r$ , is calculated using  $t_r = \frac{t-t_c}{t_c}$  where  $t$  is the time data are collected and  $t_c$  is the critical degradation time. (a, e) Data collected at  $t_r = -0.32$ , which is before degradation. Initial probe diffusivity is low and the system is rheologically and spatially homogeneous. (b, d) Data measured at  $t_r = 0.23$ , which is after  $t_c$ , where network rearrangement takes place. Since this is during rearrangement when a sample-spanning network is reformed, a lower value of probe diffusivity is measured. Both rheological and spatial heterogeneity are low. (c, g) Data collected after network rearrangement and before complete degradation at  $t_r = 0.28$ . There are a few particles in this data that have lower diffusivities and this is likely due to polymeric clusters that have not yet degraded. This sample has a small amount of rheological heterogeneity and is spatially homogeneous. (e, h) At  $t_r = 0.45$ , the sample has degraded completely. This sample is spatially and rheologically homogeneous.

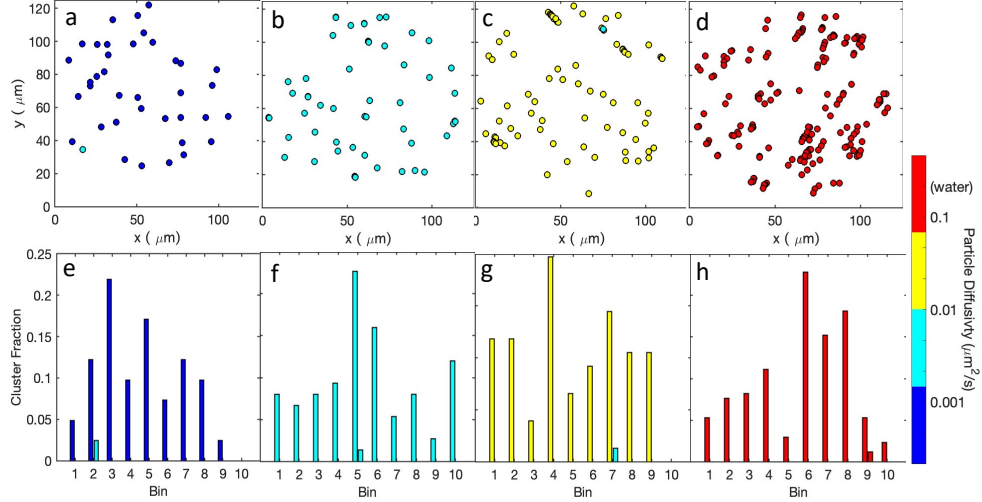


Fig. S17: (a-d) Rheological and (e-h) spatial heterogeneity in the microenvironments particles are probing during degradation of 50% excess thiol. (a-d) Particle diffusivity is plotted at the starting position of the probe particle, color indicates the diffusivity. (e-h) Histograms of the diffusivity of probe particles along the  $x$ -axis, measuring spatial heterogeneity. Each bin is  $12.5 \mu\text{m}$  in size. Each column of probe diffusivity and spatial heterogeneity is measured at a different time relative to the critical degradation time. This relative time,  $t_r$ , is calculated using  $t_r = \frac{t-t_c}{t_c}$  where  $t$  is the time data are collected and  $t_c$  is the critical degradation time. (a, e) Data collected at  $t_r = -0.38$ , which is before degradation. Initial probe diffusivity is low and the system is rheologically and spatially homogeneous. (b, d) Data measured at  $t_r = 0.26$ , which is after  $t_c$ , where network rearrangement takes place. Since this is during rearrangement when the material can reform polymer clusters but a sample-spanning network does not form, a moderate value of probe diffusivity is measured because these networks form sample-spanning networks. Both rheological and spatial heterogeneity is low. (c, g) Data collected after network rearrangement and before complete degradation at  $t_r = -0.33$ . There are a few particles in this data that have lower diffusivities and this is likely due to polymeric clusters that have not yet degraded. This sample has a small amount of rheological heterogeneity and is spatially homogeneous. (e, h) At  $t_r = 0.5$ , the sample has degraded completely. This sample is spatially and rheologically homogeneous.



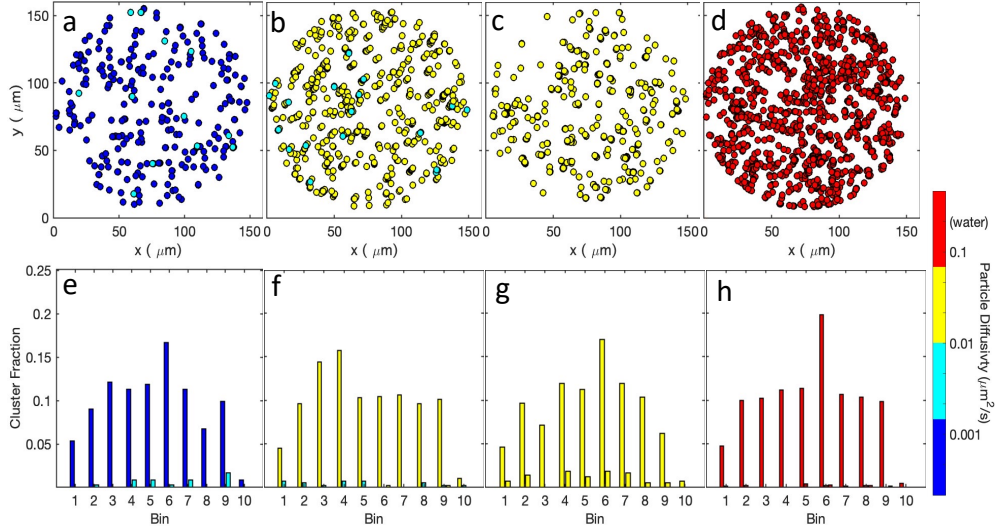


Fig. S18: (a-d) Rheological and (e-h) spatial heterogeneity in the microenvironments particles are probing during degradation of 100% excess thiol. (a-d) Particle diffusivity is plotted at the starting position of the probe particle, color indicates the diffusivity. (e-h) Histograms of the diffusivity of probe particles along the  $x$ -axis, measuring spatial heterogeneity. Each bin is  $16 \mu\text{m}$  in size. Each column of probe diffusivity and spatial heterogeneity is measured at a different time relative to the critical degradation time. This relative time,  $t_r$ , is calculated using  $t_r = \frac{t-t_c}{t_c}$  where  $t$  is the time data are collected and  $t_c$  is the critical degradation time. (a, e) Data collected at  $t_r = -0.68$ , which is before the degradation. Initial probe diffusivity is low. We do measure a small amount of rheological and spatial heterogeneity. This is likely due to the large amount of exchange reactions taking place. (b, d) Data measured at  $t_r = 0.33$ , which is after  $t_c$ , where network rearrangement takes place. Both rheological and spatial heterogeneity is measured but is relatively low. (c, g) Data collected after network rearrangement and before complete degradation at  $t_r = 0.42$ . This sample has no rheological or spatial heterogeneity. (e, h) At  $t_r = 0.73$ , the sample has degraded completely. This sample is spatially and rheologically homogeneous.

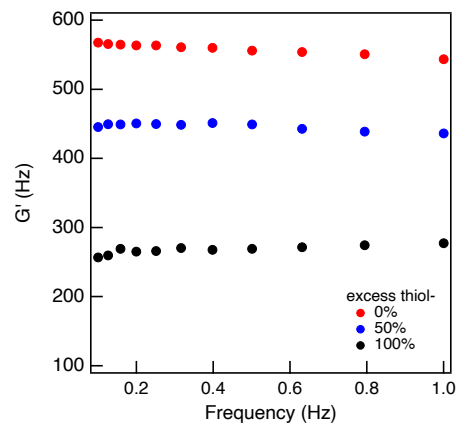


Fig. S19: Storage modulus,  $G'$ , of thioester networks is measured using frequency sweep measurements at 1% strain.